Article

A Maximum Power Transfer Tracking Method for WPT Systems with Coupling Coefficient Identification Considering Two-Value Problem

Xin Dai * [ID], Xiaofei Li [ID], Yanling Li, Pengqi Deng [ID] and Chunsen Tang

College of Automation, Chongqing University, Chongqing 400044, China; xiaofea_lee@163.com (X.L.);
20151302010@cqu.edu.cn (Y.L.); 15922949351@163.com (P.D.); cstang@cqu.edu.cn (C.T.)
* Correspondence: daixin@cqu.edu.cn; Tel.: +86-23-65112570

Abstract: Maximum power transfer tracking (MPTT) is meant to track the maximum power point during the system operation of wireless power transfer (WPT) systems. Traditionally, MPTT is achieved by impedance matching at the secondary side when the load resistance is varied. However, due to a loosely coupling characteristic, the variation of coupling coefficient will certainly affect the performance of impedance matching, therefore MPTT will fail accordingly. This paper presents an identification method of coupling coefficient for MPTT in WPT systems. Especially, the two-value issue during the identification is considered. The identification approach is easy to implement because it does not require additional circuit. Furthermore, MPTT is easy to realize because only two easily measured DC parameters are needed. The detailed identification procedure corresponding to the two-value issue and the maximum power transfer tracking process are presented, and both the simulation analysis and experimental results verified the identification method and MPTT.

Keywords: maximum power transfer tracking (MPTT); wireless power transfer (WPT); coupling coefficient; identification; impedance matching

1. Introduction

Wireless power transfer (WPT) has made a great development in the past few decades. It has been used in many occasions without the direct electrical contact (e.g., smart phone charging, implantable device charging, and electric vehicle (EV) charging, etc.) [1–8]. In a practical WPT application, usually the windings of the primary side and secondary side are compensated to degrade the input VA rating and improve the output power capacity [9–11]. Usually the operation frequency is designed to be the same with the natural frequency of the compensating resonant network to reduce the EMI [12,13]. However, one feature about the WPT system is that the load characteristic and the mutual inductance can affect the resonant frequency, so the power transfer capability and the system efficiency will be influenced accordingly [14,15].

Maximum power transfer (MPT) is an important performance index of WPT system, which can indicate the maximum power transfer capacity [1,16]. Traditionally, impedance matching method is utilized to realize the maximum power transfer tracking (MPTT) [17]. Reference [18] realizes the impedance matching by adding passive components while references [5,19–21] do the impedance matching through DC/DC converters (e.g., Boost, Buck, Sepic, etc.). Since the load resistance of a practical WPT system varies with time, therefore using DC/DC converters to do the impedance matching is more suitable for the frequent load variations [19]. However, one thing about the impedance matching using DC/DC converters is that it cannot be realized when unknowing the parameters, such as coupling coefficient and load resistance [22,23]. Therefore, in order to achieve MPTT, the identification of these changing parameters is needed previously.

Some researchers have done the related works on the load and coupling coefficient identification. Reference [14] presents a coupling coefficient and load identification method, with two equations derived by switching the compensation capacitors, the two variables can be calculated. However, the equations require the information of the resonant currents on primary and secondary sides, which will increase the difficulty in practice. References [22,23] present a dynamical identification method of coupling coefficient, and it only need to measure the parameters on the secondary side. However, it needs to measure the RMS value of alternating currents, which will bring harmonic interference. In addition, the continuous and discontinuous operation modes will influence the accuracy of the modeling. Reference [24] also studies the identification of mutual inductance and load resistance. These two parameters can be calculated under one operating frequency condition with the front-end monitoring method. However, the high estimation accuracy will sacrifice the system efficiency.

This paper presents an identification method of coupling coefficient for MPTT in WPT system. The method does not require any other circuit to implement the identification and the identification only need to measure two DC parameters on secondary side. Especially, the two-value issue during the identification process is solved. As long as the coupling coefficient and load are determined, the maximum power transfer tracking is realized by impedance matching. The paper is structured as follows: system topology, coupling coefficient identification, and MPTT description is presented in Section 2, system parameters and the simulation analysis are shown in Section 3, experimental verification of the proposed coupling coefficient identification and the MPTT are shown in Section 4, and the conclusions are presented in Section 5.

2. Coupling Coefficient Identification and Maximum Power Transfer Tracking

2.1. System Topology

Figure 1 shows the schematic circuit of the proposed tracking topology, where the input DC voltage is given by E, R_b is the load resistance. R_p and R_s are the internal resistance of L_p and L_s, respectively. L_p, C_p constitute the primary series resonant circuit, while L_s, C_s constitute the secondary series resonant circuit. M is the mutual inductance, and satisfies $M = k\sqrt{L_p L_s}$ (k represents the coupling coefficient). $S_1 \sim S_4$ constitute the full-bridge inverter, while $D_1 \sim D_4$ constitute the rectifier. S_b, D_b, L_b, C_b constitute the Buck converter. R_{bin} and R_{rin} are the equivalent input impedances of the Buck converter and rectifier circuit, respectively. i_p and i_s are the resonant currents. V_s, V_r, U_b are the input voltage of the resonant circuit, the rectifier and the Buck converter respectively. To reduce EMI, assuming the operating frequency f of the inverter is same with the nature frequency of the resonant circuit, i.e., $f = \frac{1}{2\pi\sqrt{L_p C_p}} = \frac{1}{2\pi\sqrt{L_s C_s}}$.
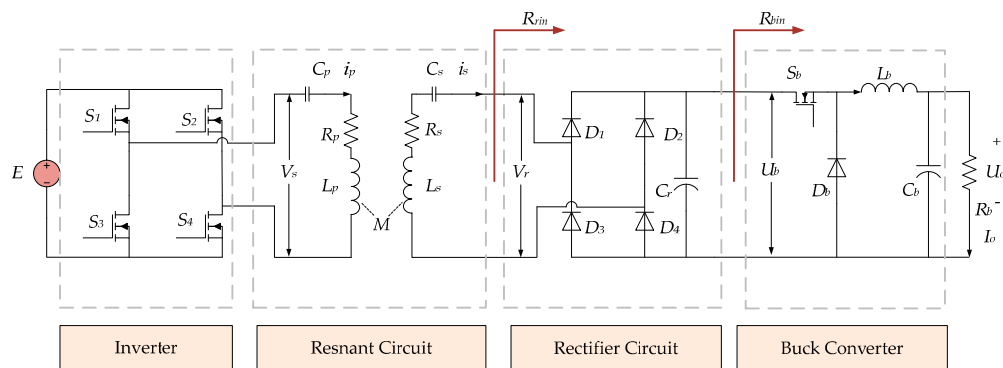

Figure 1. Schematic circuit of the tracking topology.

2.2. Identification of the Coupling Coefficient

Assuming that there is no power loss in the rectifier, the relationship between the input and output resistance is:

$$R_{rin} = \frac{8}{\pi^2} R_{bin}. \tag{1}$$

As for the relationship between the input and output resistance of the Buck converter, it can also be derived. Take the continuous conduction mode (CCM) operation of Buck converter into consideration, the relationship between R_{bin} and R_b is:

$$R_{bin} = \frac{R_b}{d^2} \tag{2}$$

where d indicates the duty cycle of the Buck converter, and d should satisfy: $\frac{2L_b}{R_b T_b} > 1 - d$ to achieve the CCM operation of Buck converter. R_b can be derived by $\frac{U_o}{I_o}$.

It is found that the theoretical model of the secondary circuit (i.e., resonant circuit, rectifier, and Buck converter) is more precisely when the secondary resonant current i_s is continuous. Figure 2 is presented to show a case of continuous current. i_s is continuous with the following condition [25]:

$$R_{bin} \leq \frac{\pi \omega L_s}{4} \rightarrow d \geq \sqrt{\frac{4R_b}{\pi \omega L_s}}. \tag{3}$$

where ω is the angular frequency of the resonant circuits, and satisfies $\omega = \frac{1}{\sqrt{L_p C_p}} = \frac{1}{\sqrt{L_s C_s}}$.
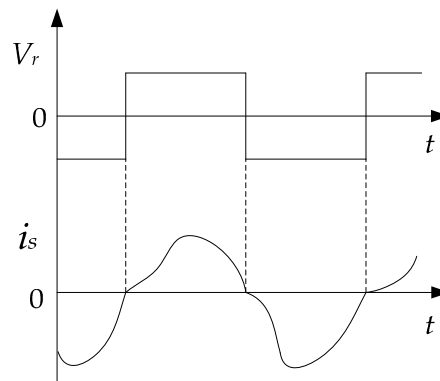
Figure 2. Continuous current condition waveforms of the system.

By calculating Equations (1) and (2), the following relationship can be derived:

$$R_b = \frac{\pi^2 d^2}{8} R_{rin}. \tag{4}$$

The RMS value of i_p is:

$$I_p = \frac{U_s}{R_p + Z_{ref}} \tag{5}$$

where U_s is the RMS value of V_s satisfying $U_s = \frac{2\sqrt{2}}{\pi} E$. Z_{ref} is the reflected impedance, satisfies $Z_{ref} = \frac{\omega^2 M^2}{R_{rin} + R_s}$.

The RMS value of V_r is:

$$U_r = \omega M I_p \frac{R_{rin}}{R_{rin} + R_s}. \tag{6}$$

Therefore, the output voltage U_o can be calculated as:

$$U_o = \frac{\sqrt{2}\pi d}{4} U_r. \tag{7}$$

By calculating (7), the relationship between k and the measured U_o can be derived as:

$$k = \frac{4ER_b \pm \sqrt{16E^2 R_b^2 - \pi^4 R_p R_s U_o^2 d^2 - 8\pi^2 R_b R_p U_o^2}}{\sqrt{L_p L_s} \pi^2 \omega d U_o}. \tag{8}$$

E, ω, d, L_p, L_s, R_p, and R_s are the known parameters. k can be calculated from (8) with the measured DC parameters U_o and I_o. However, Equation (8) shows that derivation of k may have two values based on one instance of U_o. Therefore, at least two instances of output voltage are needed to identify the actual k. In the next part, this two-value issue during the identification will be solved.

2.3. Dealing with the Two-Value Issue When Identifing the Coupling Coefficient

Figure 3 is presented here to indicate the identification process when considering the two-value issue.
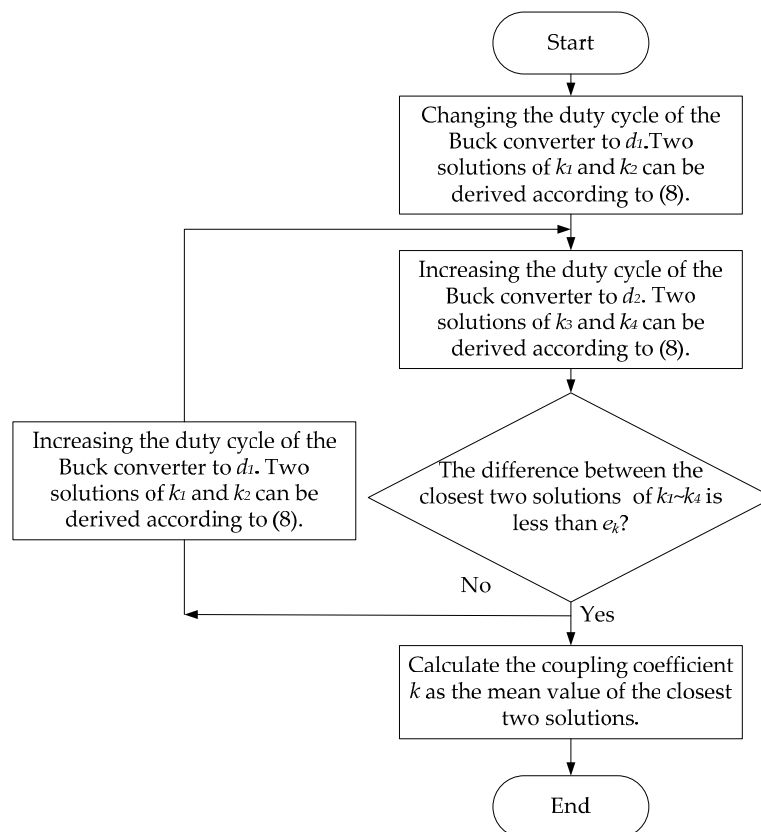
Figure 3. Flowchart of the identification process when considering the two-value issue.

During the identification process, by changing the duty cycle twice, two instances of U_o can be derived. By calculating Equation (8), four solutions of coupling coefficient can be obtained. Then compare the four solutions if there is a difference between two solutions is less than the tolerance error e_k. The actual coupling coefficient can be determined by calculating the mean value of these two solutions. Otherwise, we will increase the duty cycle and restart the identification process. It should be noted that we just need the identification of the coupling coefficient once before the maximum power tracking process when there is no relative movement between the primary and

secondary coils. When the coupling coefficient is identified, the maximum power tracking can be achieved through impedance matching and this will be introduced in the following section.

2.4. Maximum Power Transfer Tracking

Take a series-series (SS) topology WPT system shown in Figure 4 as example. The coupling equations can be derived as:

$$\begin{cases} V_s = (R_p + jX_p)i_p - j\omega M i_s \\ 0 = (R_s + jX_s)i_s - j\omega M i_p \end{cases} \tag{9}$$

where $X_p = \omega L_p - \frac{1}{\omega C_p}$ and $X_s = \omega L_s - \frac{1}{\omega C_s}$. When the operating frequency equals to the natural frequency of the resonant circuits (i.e., $X_p = 0$; $X_s = 0$), the output power P_L can be derived as:

$$P_L = I_s{}^2 R_L = \frac{\omega^2 M^2 U_s^2 R_L}{\left(\omega^2 M^2 + R_p R_s + R_p R_L\right)^2} \tag{10}$$

where, I_s is the RMS value of i_s, U_s is the RMS value of V_s.

The maximum power transfer point corresponding to the load resistance can be solved by $\frac{\partial P_L}{\partial R_L} = 0$, the optimum resistance is:

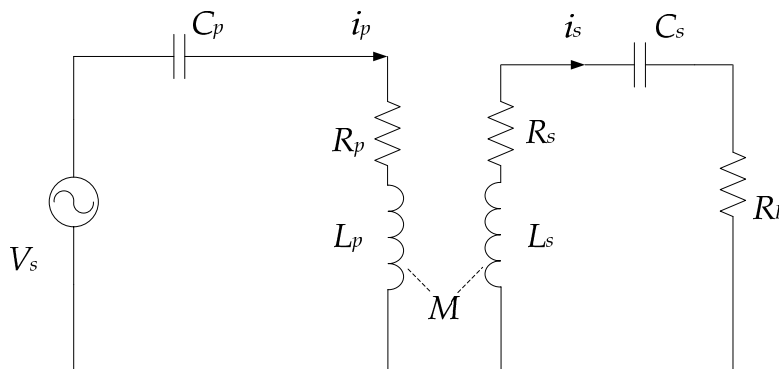$$R_{L-P_{\max}} = R_s \left(1 + \frac{\omega^2 M^2}{R_p R_s}\right). \tag{11}$$

The maximum output power is:

$$P_{\max} = \frac{\omega^2 M^2 U_s^2 R_{L-P_{\max}}}{\left(\omega^2 M^2 + R_p (R_s + R_{L-P_{\max}})\right)^2} \tag{12}$$

System efficiency (given by the output power divided by input power) at the maximum power transfer point is:

$$\eta = \frac{I_s^2 R_{L-P_{\max}}}{I_p^2 R_p + I_s^2 R_{L-P_{\max}} + I_s^2 R_s} = \frac{\omega^2 M^2 R_{L-P_{\max}}}{\left(\omega^2 M^2 + R_p (R_s + R_{L-P_{\max}})\right)(R_s + R_{L-P_{\max}})} \tag{13}$$

where I_p is the RMS value of i_p.

Figure 4. Primary and secondary series-series (SS) resonant wireless power transfer (WPT) topology.

As is mentioned before, the load resistance of the WPT system may change during the whole power transfer process, and the transferred power will change accordingly. As the tracking topology shown in Figure 1, a Buck converter is utilized to track the maximum power point. MPTT can be realized through changing the duty cycle of the Buck converter. By calculating Equations (4) and (11), the optimum duty cycle d_{opt} can be derived:

$$d_{opt} = \frac{2\sqrt{2R_{L-P_{\max}}R_b}}{\pi R_{L-P_{\max}}}.$$
(14)

Figure 5 shows the flowchart of the maximum power transfer tracking process. After the identification of the coupling coefficient and the load resistance, MPTT can be realized through impedance matching (i.e., changing the duty cycle of the Buck converter). Load R_b is detected during the whole charging process. If R_b is varied, the optimum duty cycle d derived by Equation (14) will fed to the Buck converter.
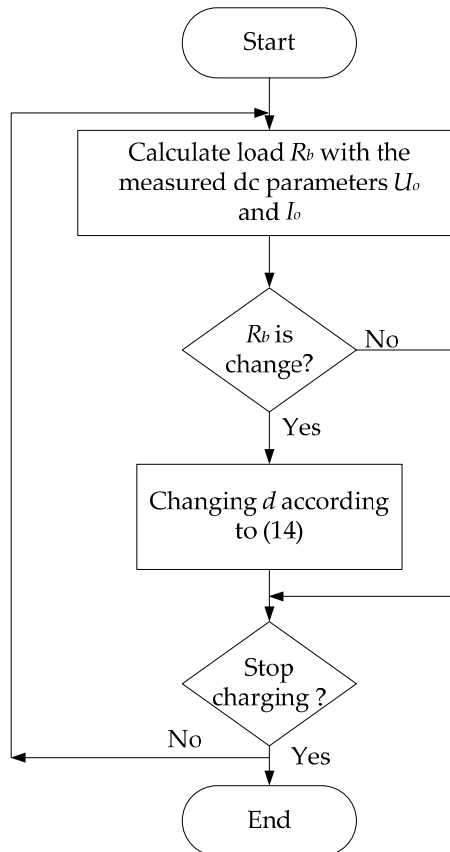

Figure 5. Flowchart of the maximum power transfer tracking.

3. Simulation Analysis

3.1. System Parameters and the Control Structure

In this section, the presented identification approach and MPTT will be verified by Matlab/Simulink. With the parameters shown in Table 1 and the topology shown in Figure 1, a simulation model is built. The parameters of the Litz-wire coils indicate the item used in experiment. f_b is the frequency of the Buck converter.

Figure 6 shows the control structure diagram. The detection unit detects the DC output voltage and current on the secondary side. The controller identifies the coupling coefficient and control the duty cycle of the Buck converter to track the maximum power.

Table 1. Parameters of the system.

Items	Parameter	Value	Parameter	Value
Resonant circuits	L_p	365.96 µH	L_s	363.68 µH
	R_p	0.83 Ω	R_s	0.51 Ω
	C_p	34.25 nF	C_s	34.30 nF
Litz-wire coils	*Diameter*	14 cm	*Number of turns*	25
Frequencies	*f*	45 kHz	f_b	100 kHz
Buck converter	L_b	120 µH	C_b	470 µF
Input source	*E*	10 V		
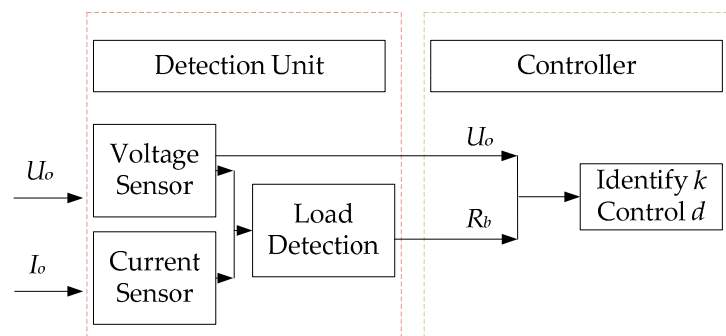
Figure 6. The control structure of the proposed method.

3.2. Analysis of the Coupling Coefficient Identification and Maximum Power Transfer Tracking

As mentioned before, the theoretical model of the secondary side circuit will be more precise when i_s is continuous. According to Equation (3) and the parameters shown in Table 1, we can derive that when *d* is larger than 0.3, the current is continuous. Figure 7 shows the identification accuracies of the coupling coefficient when *d* varies from 0.2 to 0.9. The reference *k* is selected as 0.15 while $R_b = 10$ Ω.
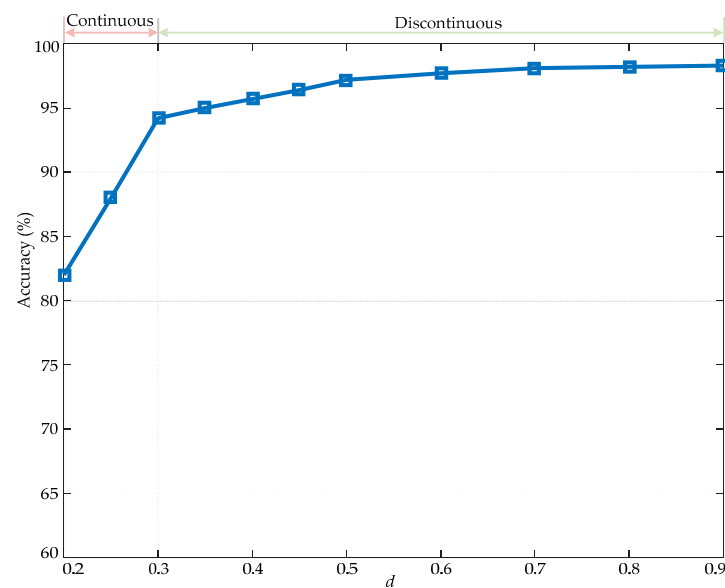

Figure 7. Identification accuracies of coupling coefficient when *d* varies from 0.2 to 0.9.

Figure 7 shows that when *d* is larger than 0.3 (i.e., i_s is continuous), the identification accuracies are all larger than 95%, while the identification accuracies are below 90% when i_s is discontinuous. Therefore, only the continuous current case is taken into consideration in this paper.

Table 2 shows the coupling coefficient identification results when the reference *k* varies, where the load resistance R_b is set at 10 Ω, $d_1 = 0.5$, $d_2 = 0.6$, $e_k = 0.0027$. The identification accuracy is over 94% at all of the coupling coefficient conditions. These high accuracy identification results indicate that the identification method is feasible.

Table 2. Coupling coefficient identification with *d* is 0.5, 0.6 and R_b is 10 Ω.

| Reference *k*	Identified *k*	Accuracy
0.0448	0.0474	94.16%
0.0811	0.0839	96.59%
0.0930	0.0962	96.67%
0.1500	0.1531	97.93%
0.2000	0.2037	98.15%
0.2500	0.2546	98.16%

As for the MPTT of the system, the simulation results are shown in Figure 8. R_b changes from 10 to 30 Ω, and two coupling coefficient cases are considered (the given coupling coefficients are 0.0448 and 0.0811, while the identified coupling coefficients are 0.0474 and 0.0839). The theoretical maximum power can be derived from (12), which are shown in the top of Figure 8a,b with dot line. The middle of the figure indicates the practical output power while the load R_b variation is shown in the bottom of the figure. Both the two figures (a) and (b) share the similar features, due to the identification error of *k* and the non-ideal of the semiconductor switch and diode, the practical output power is slightly lower than the theoretical value. The steady state of the practical output power (P_o) is almost the same at different load condition, this can prove that the maximum power tracking is achieved. At the changing instant of load R_b, the practical output power is pulsatile due to the switch noise, and it cannot be totally eliminated.
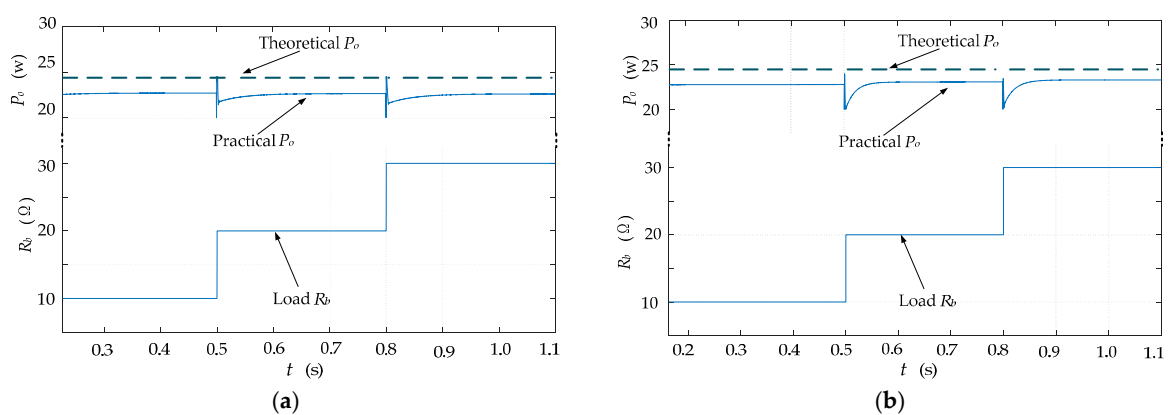
Figure 8. Maximum power tracking when load R_b changes with different *k*: (**a**) *k* = 0.0811; (**b**) *k* = 0.0448.

System efficiencies at steady state under these two coupling coefficients are shows in Figure 9. In general, the output power is at its maximum when the external resistance is equal to the internal resistance, so the efficiency under the maximum power transfer condition is close to 50%.
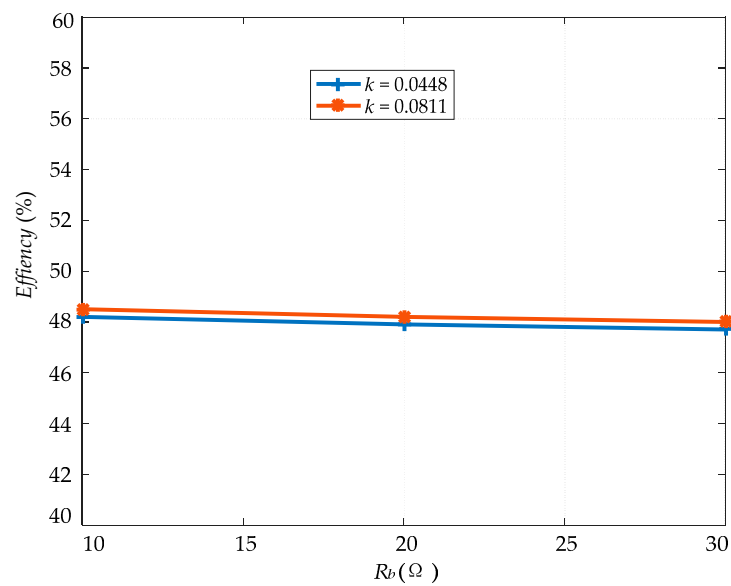
Figure 9. Simulation analysis of system efficiencies under maximum power transfer tracking (MPTT) condition.

4. Experimental Analysis

4.1. Experimental Setup

An experimental setup is built to verify the proposal. The experimental system topology is same with Figure 1 and Table 1 gives its parameters. In the experiment, the primary and secondary coils are in same configuration and wound by Litz wires. The diameter of the coil is 14 cm, while the number of turns is 25. Figure 10 shows the photo of the experimental setup, where an ARM chip is used as the detection unit to measure the DC voltage and current, while an FPGA chip is selected as the controller. The variable load is achieved by switching the relay array.
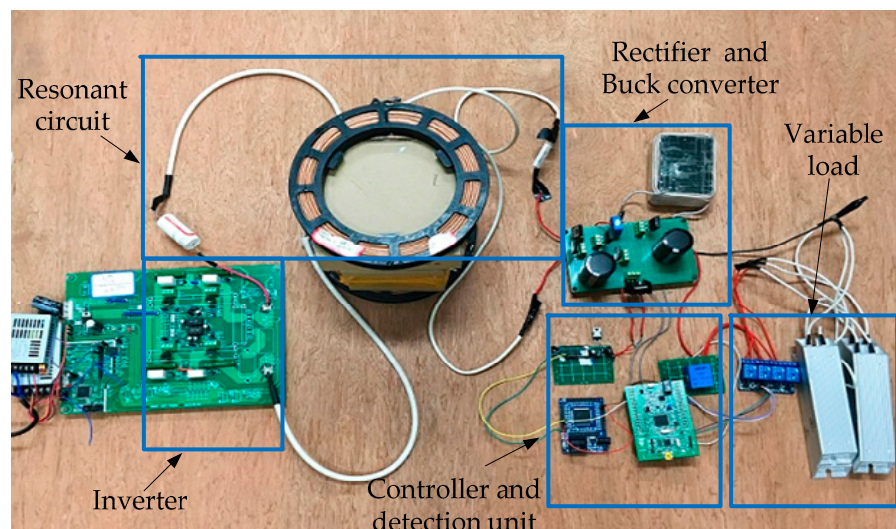
Figure 10. The experimental setup.

4.2. Experimental Results

As is indicated before, *k* is firstly need to be identified before the maximum power tracking. Since there are two solutions with respect to one voltage U_o, as shown in Equation (8), so we need to

motivate the system twice by changing d as shown in Figure 3. When there is difference lower than e_k between two solutions, k can be calculated by averaging these two solutions. e_k should be selected as a small value to ensure the high identification accuracy, in this paper we choose e_k to be 0.0027 (i.e., the mutual inductance is 1 μH). One thing about the selecting of d is that, as can be seen from Figure 7, the identification accuracy is relatively higher when d is larger until d increase to a certain value. Therefore, when k cannot be identified, we just increase d as shown in Figure 3.

In order to verify the identification method of the coupling coefficient, we firstly measure two reference coupling coefficients under two alignment conditions of the coupling coils, the two values are 0.0811 and 0.0448 while the separation distance between the couplers are 6 cm and 9 cm, respectively. The identification process and the results are shown in Table 3.

Table 3. Identification process and results of k.

Separation Distance	Reference k	Motivating d_1	Motivating d_2	Identified k	Accuracy
6 cm	0.0811	$d_1 = 0.5$ $k_1 = 0.0877; k_2 = 0.0183$	$d_2 = 0.6$ $k_3 = 0.0854; k_4 = 0.0098$	0.0866	93.2%
9 cm	0.0448	$d_1 = 0.5$ $k_1 = 0.0484; k_2 = 0.0332$	$d_2 = 0.6$ $k_3 = 0.0464; k_4 = 0.0207$	0.0474	94.2%

As shown in Table 3, the identification of the two reference coupling coefficients 0.0811 and 0.0448 can be determined when d_1 and d_2 are selected as 0.5 and 0.6. k_1 and k_3 has the difference lower than e_k, so the identification of k can be determined, and the accuracies of the two conditions are higher than 93%.

After the identification of k, MPTT can be achieved. We change the load resistance R_b at 10, 20, and 30 Ω. ARM chip can detect the load variation, and then the tracking duty cycle d can be calculated by Equation (14). The maximum power tracking results under the two coupling conditions are shown in Figure 11, where the values in the blue rectangular boxes indicate the measured output power P_o, I_o, and U_o under different load and coupling conditions.


(a)

Figure 11. *Cont.*

(b)
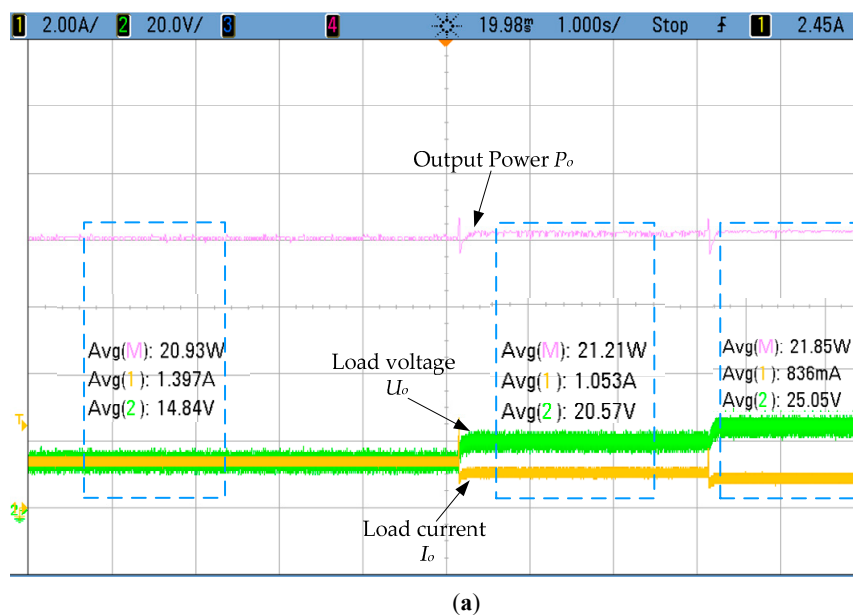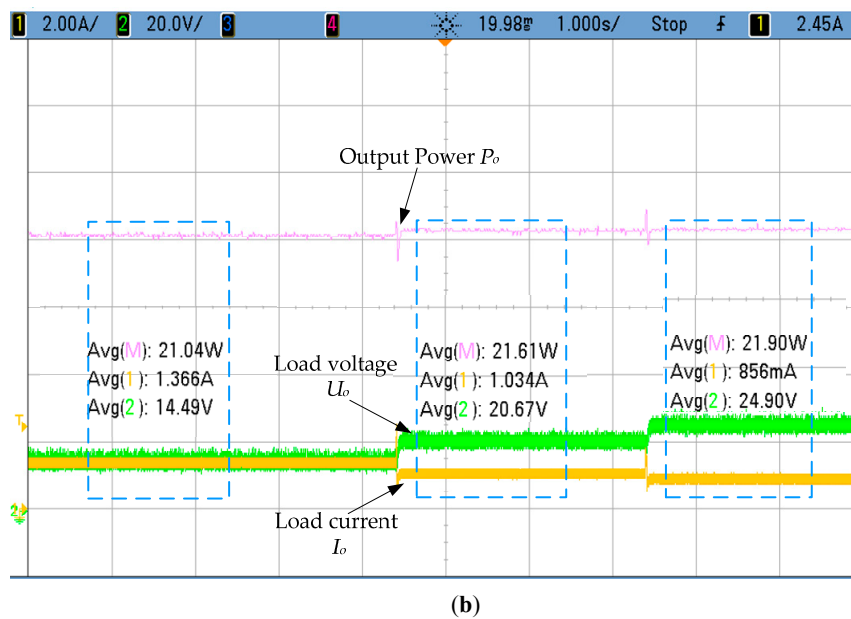
Figure 11. Experimental MPTT results when load R_b changes with different k: (**a**) $k = 0.0811$; (**b**) $k = 0.0448$.

The top of the figure shows the practical output power, while the bottom of the figure shows the detected voltage U_o and current I_o. By comparing Figure 11a,b and Figure 8a,b the experimental output power is slightly smaller than the simulation results because of the identification error of k and the losses in the experiment system. When load R_b changes, the tracked maximum output power is almost the same at the steady state, this can prove that the maximum power tracking is achieved.

System efficiencies under the MPTT condition are shown in Figure 12. The results are less than that of simulation results, partly due to the disturbance in the experiment.
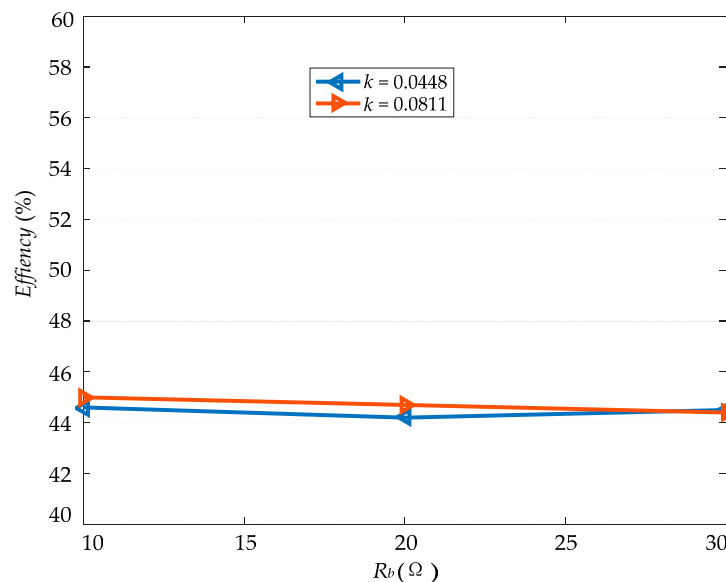
Figure 12. Experimental analysis of system efficiencies under MPTT condition.

These experimental results verified the proposed identification approach and MPTT method. It should be noted that there are always some errors during the experimental measurements, thus the identification accuracy and the maximum power are lower than the simulation results, to further improve the experimental accuracy, the improved filtering algorithms and circuits can be used to

reduce the measurement errors. Furthermore, the semiconductor switching loss is ignored when calculating the theoretical output power, so both the simulation and the experimental output power are lower than the theoretical results. Besides, in this paper, we just consider the variations of the load resistance, other variations of the system parameters are very small during the power transfer, so the interference is very small.

The coupling coefficient identification is required only once before the maximum power transfer tracking process when there is no relative movement between the primary and secondary couplers, and the required parameters are all in steady state. The identification time of the coupling coefficient is about 30 ms, while the detection time of R_b is about 10 ms in steady state. After the identification of k, the maximum power transfer tracking can be done through impedance matching. As for the changing of load R_b, the gap time between the two variable loads just need to be larger than the identification time. The proposed identification method shown in Figure 3 is also suitable for the dynamical identification of the coupling coefficient, and the variation of the coupling coefficient should be slower enough for the coupling coefficient identification.

5. Conclusions

This paper presents a maximum power transfer tracking method in WPT systems with coupling coefficient identification. A two instance determination method is given to prevent two-value issue during the identification. The identification algorithm is also presented in detail to realize MPTT. When compared with other identification method, the proposed method only needs the DC variable measurements and it does not need any other circuit except for the inherent MPTT circuit. After the identification of the coupling coefficient and load resistance, MPTT is realized by impedance matching. Both the simulation and experimental results have verified the identification approach and the MPTT method.

Author Contributions: Xiaofei Li and Pengqi Deng designed and performed the experiments; Xiaofei Li, Xin Dai and Chunsen Tang analyzed the experimental data and wrote the paper; all of the authors have done the editing and proofreading of this paper.

Conflicts of Interest: The authors declare no conflicts of interest.

References

1. Dai, X.; Li, X.F.; Li, Y.L.; Hu, A.P. Impedance Matching Range Extension Method for Maximum Power Transfer Tracking in IPT System. *IEEE Trans. Power Electron.* **2017**. [CrossRef]
2. Jawad, A.M.; Nordin, R.; Gharghan, S.K.; Jawad, H.M.; Ismail, M. Opportunities and Challenges for Near-Field Wireless Power Transfer: A Review. *Energies* **2017**, *10*, 1022. [CrossRef]
3. Jiang, C.; Chau, K.T.; Liu, C.; Lee, C.H.T. An Overview of Resonant Circuits for Wireless Power Transfer. *Energies* **2017**, *10*, 894. [CrossRef]
4. Dai, X.; Jiang, J.; Li, Y.; Yang, T. A Phase-Shifted Control for Wireless Power Transfer System by Using Dual Excitation Units. *Energies* **2017**, *10*, 1000. [CrossRef]
5. Zhong, W.X.; Hui, S.Y.R. Maximum Energy Efficiency Tracking for Wireless Power Transfer Systems. *IEEE Trans. Power Electron.* **2015**, *30*, 4025–4034. [CrossRef]
6. Covic, G.A.; Boys, J.T. Inductive Power Transfer. *Proc. IEEE* **2013**, *101*, 1276–1289. [CrossRef]
7. Hui, S.Y.R.; Zhong, W.X.; Lee, C.K. A Critical Review of Recent Progress in Mid-Range Wireless Power Transfer. *IEEE Trans. Power Electron.* **2014**, *29*, 4500–4511. [CrossRef]
8. Wei, X.; Wang, Z.; Dai, H. A Critical Review of Wireless Power Transfer Via Strongly Coupled Magnetic Resonances. *Energies* **2014**, *7*, 4316–4341. [CrossRef]
9. Li, W.; Zhao, H.; Li, S.; Deng, J.; Kan, T.; Mi, C.C. Integrated LCC Compensation Topology for Wireless Charger in Electric and Plug-In Electric Vehicles. *IEEE Trans. Ind. Electron.* **2015**, *62*, 4215–4225. [CrossRef]

10. Zhang, W.; Mi, C.C. Compensation Topologies of High-Power Wireless Power Transfer Systems. *IEEE Trans. Veh. Technol.* **2016**, *65*, 4768–4778. [CrossRef]

11. Wang, C.S.; Covic, G.A.; Stielau, O.H. Power Transfer Capability and Bifurcation Phenomena of Loosely Coupled Inductive Power Transfer Systems. *IEEE Trans. Power Electron.* **2004**, *51*, 148–157. [CrossRef]

12. Pawellek, A.; Oeder, C.; Duerbaum, T. Comparison of Resonant LLC and LCC Converters for Low-Profile Applications. In Proceedings of the 14th European Conference on Power Electronics and Applications (EPE)/ECCE Europe Conference on Power Electronics and Adjustable Speed Drives, Birmingham, UK, 30 August 1–September 2011; pp. 1–10.

13. Li, X.F.; Tang, C.S.; Dai, X.; Deng, P.Q.; Su, Y.G. An Inductive and Capacitive Combined Parallel Transmission of Power and Data for Wireless Power Transfer Systems. *IEEE Trans. Power Electron.* **2017**. [CrossRef]

14. Su, Y.G.; Zhang, H.Y.; Wang, Z.H.; Hu, A.P.; Chen, L.; Sun, Y. Steady-State Load Identification Method of Inductive Power Transfer System Based on Switching Capacitors. *IEEE Trans. Power Electron.* **2015**, *30*, 6349–6355. [CrossRef]

15. Dai, X.; Li, X.F.; Li, Y.L.; Hu, A.P. Maximum Efficiency Tracking for Wireless Power Transfer Systems with Dynamic Coupling Coefficient Estimation. *IEEE Trans. Power Electron.* **2017**. [CrossRef]

16. Liu, Y.; Hu, A.P.; Madawala, U.K. Maximum Power Transfer and Efficiency Analysis of Different Inductive Power Transfer Tuning. In Proceedings of the 10th IEEE Conference on Industrial Electronics and Applications, Auckland, New Zealand, 15–17 July 2015; pp. 655–660.

17. Li, H.L.; Hu, A.P.; Covic, G.A.; Tang, C.S. Optimal Coupling Condition of IPT System for Achieving Maximum Power Transfer. *Electron. Lett.* **2009**, *45*, 76–77. [CrossRef]

18. Xiao, C.; Liu, Y.; Cheng, D.; Wei, K. New Insight of Maximum Transferred Power by Matching Capacitance of a Wireless Power Transfer System. *Energies* **2017**, *10*, 688. [CrossRef]

19. Zhong, W.X.; Hui, S.Y.R. Maximum Energy Efficiency Operation of Series-Series Resonant Wireless Power Transfer Systems Using On-Off Keying Modulation. *IEEE Trans. Power Electron.* **2017**. [CrossRef]

20. Li, H.C.; Li, J.; Wang, K.; Chen, W.; Yang, X. A Maximum Efficiency Point Tracking Control Scheme for Wireless Power Transfer Systems Using Magnetic Resonant Coupling. *IEEE Trans. Power Electron.* **2015**, *30*, 3998–4008. [CrossRef]

21. Fu, M.F.; Ma, C.; Zhu, X. A Cascaded Boost-Buck Converter for High-Efficiency Wireless Power Transfer Systems. *IEEE Trans. Ind. Inf.* **2014**, *10*, 1972–1980. [CrossRef]

22. Kobayashi, D.; Imura, T.; Hori, Y. Real-time Coupling Coefficient Estimation and Maximum Efficiency Control on Dynamic Wireless Power Transfer for Electric Vehicles. In Proceedings of the IEEE PELS Workshop on Emerging Technologies: Wireless Power (WoW), Daejeon, Korea, 5–6 June 2015; pp. 1–6.

23. Jiwariyavej, V.; Imura, T.; Hori, Y. Coupling Coefficients Estimation of Wireless Power Transfer System via Magnetic Resonance Coupling Using Information from Either Side of the System. *IEEE J. Emerg. Sel. Topics Power Electron.* **2014**, *3*, 191–200. [CrossRef]

24. Yin, J.; Parisini, T.; Hui, S.Y. Front-End Monitoring of the Mutual Inductance and Load Resistance in a Series–Series Compensated Wireless Power Transfer System. *IEEE Trans. Power Electron.* **2016**, *31*, 7339–7352. [CrossRef]

25. Forsyth, A.J.; Ward, G.A.; Mollow, S.V. Extended Fundamental Frequency Analysis of the LCC Resonant Converter. *IEEE Trans. Power Electron.* **2003**, *18*, 1286–1292. [CrossRef]